Chapter 2
Literature Review

2.1 Thermal Properties

2.1.1 Specific heat

Specific heat, which represents the heat capacity of concrete, is little affected by the mineralogical characteristic of the aggregate, but is considerably increased by an increase in the moisture content of the concrete (Neville 1995). The specific heat of concrete is determined by elementary methods of physics. During the hydration process the specific heat changes with respect to time. The amount of free water in concrete decreases with an increase in the degree of hydration. As the specific heat of water is the highest among all other ingredients of concrete, specific heat of concrete is considered to decrease rapidly at the early stage of hydration along with the decrease in the amount of free water. The specific heat is a parameter used to relate the hydration heat generated in the concrete and its temperature rise as shown in Eq. (2.1).

$$Q = \int H dt = mc\Delta T \tag{2.1}$$

where Q is the cumulative heat of hydration (kcal), H is heat generation rate per unit solid volume of concrete, and c is the specific heat of concrete (kcal/kg/°C). ΔT is temperature rise at time t (°C), m is mass of concrete (kg), and t is age of concrete (days).

Brown and Javaid (1970) reported that the specific heat of normal strength concrete (water to binder ratio of 0.65) varied from 1.15 to 0.89 kJ/kg/°C at ages varying from 6 hours to 7 days, respectively.

Hansen et al. (1982) measured the specific heat of hardening Portland cement paste by varying water-cement ratios and temperatures. A test method for determining the specific heat during hardening was proposed. The experimental method developed is traditional in principle: the temperature rise due to a known heat input of a calorimeter with and without cement paste sample is determined. The method has been calibrated on aluminum. Specific heat was found to decrease from 1.92 ± 0.05 kJ/kg °C at 1.5 hours to 1.65 ± 0.01 kJ/kg °C at 120 hours.

Schutter and Taerwe (1995) measured the specific heat of hardening cement paste samples made with blast furnace slag cement and found that the specific heat decreased linearly with the degree of hydration. The specific heat was determined by measuring the temperature rise in the calorimeter caused by certain energy supply. Tests were carried out in a cement paste with water-cement ratio of 0.5. In order to obtain the variation of the specific heat during hardening, cement paste samples were tested at ages ranging from one day to seven days. The corresponding degree of hydration was calculated as the fraction of heat released. Until testing, the cement paste samples were stored at 20 °C and 95% relative humidity.

Xu and Chung (2000) reported that sand addition decreased the specific heat of mortars with and without silica fume by 11% and 13%, respectively when compared to those of cement pastes with and without silica fume. They also found that silica fume addition increased the specific heat of cement paste and mortar by 7% and 10%, respectively.

Jitvutikrai (2000) conducted the experiments to determine the specific heat of pastes and mortars. From the experimental results, it was found that the specific heat depended largely on the amount of free water content in the specimens. The replacement of cement by fly ash did not have much effect on specific heat at initial state but seemed to cause the reduction of specific heat in long term due to pozzolanic reaction. He also found that amount of aggregates had significant effect on specific heat, specimens with higher aggregate content possed lower specific heat than those with lower aggregate content.

2.1.2 Thermal conductivity

Thermal conductivity is the rate of heat transfer through a unit cross-sectional area of material for a unit temperature gradient. Heat conductivity is the mechanism of heat flow in which energy is transported from the region of high temperature to the region of low temperature by the drift of electrons, as in solid (Bayazitoglu and Ozisik 1988). The conduction law is based on the Fourier law. Fourier law states that the rate of heat flow by conduction in a given direction is proportional to the gradient of temperature in that direction (dT/dx) and the area normal to the direction of heat flow (A). The expression of heat flow is shown in Eq. (2.2).

$$q_x = -kA\frac{dT}{dx} \tag{2.2}$$

where k is the thermal conductivity (kcal/ m day ^oC). q_x is the rate of heat flow in x direction (kcal/day). A is the cross-sectional area normal to the direction of heat flow (m^2). dT/dx is the temperature gradient in the direction of heat flow (°C/m).

Thermal conductivity of concrete is greatly affected by the mineralogical character of the aggregate. Moisture content in concrete also affects the thermal conductivity in such a way that when the degree of saturation increases the conductivity also increases since the thermal conductivity of air is lower than that of the water. The value of thermal conductivity in concrete changes with respect to time due to the hydration process.

Brown and Javaid (1970) reported a decrease in the thermal conductivity for a conventional concrete by 30% of its initial value during a period of first seven days after casting and a subsequent constant value after that period. But their measured values showed an initial increase of the thermal conductivity. They also stated that the specific heat of hardening concrete decreased linearly with time by about 20%.

Toyokazu and Yoshiro (1976) investigated the thermal conductivity of fresh mortar and fresh concrete. They found that thermal conductivity increased during the age of 3 days and became almost constant after the age of 3 – 6 days.

Nanayakkara (2001) developed an experimental method to measure the thermal conductivity of concrete. The method involved the measurement of steady state temperature distribution across a cylindrical specimen of concrete under known heat flux supplied at the center of the specimen by a heating coil. He observed that the thermal conductivity of concrete varied with the age of concrete and also across the section of the specimen. The variation of conductivity across the section may be due to the non-uniform distribution of free water and hydrated products.

Khan (2002) investigated the thermal conductivity of mortar, concrete and its major constituent aggregate. He reported that thermal conductivity of rocks, mortar and concrete increased with an increase in the moisture content. In case of concrete, the rate of increase was more significant from dry state to 50% degree saturation, beyond which it was less significant. The type of aggregate also had significant influence on thermal conductivity of mortar and concrete.

Kim et al. (2003) investigated the influencing factors on thermal conductivity of concrete, mortar and cement paste. The variables for testing are age, w/b, type of admixtures, aggregate volume fraction, temperature and humidity condition. According to his experimental results, aggregate volume fraction and moisture condition of specimen are revealed as major affecting factors for conductivity of concrete. Meanwhile, the conductivities of mortar and cement paste are strongly affected by the w/b ratio and types of admixtures. However, age hardly changes the conductivity except at very early age. They proposed a prediction model of *k* based on the experimental results. The model took into account the effect of the volume of aggregate, concrete temperature, moisture condition and the fine aggregate fraction (s/a). The suggested expression for thermal conductivity of the concrete is shown below.

$$k = k_{ref}\left[0.293 + 1.01AG\right]\left[0.8\left(1.62 - 1.54\left(w/b\right)\right) + 0.2R_h\right]\left[1.05 - 0.0025T\right]\left[0.86 + 0.0036\left(s/a\right)\right] \quad (2.3)$$

where AG is an aggregate volume fraction in concrete. T is concrete temperature. R_h is an average relative humidity of concrete (R_h = 1.0 for saturated condition). k_{ref} is a reference *k* measured from specimens at the condition of AG=0.7, w/b =0.4, s/a = 0.4, T=20 ^oC, and R_h = 1.0 (W/m K).

Demirboğa (2003) investigated the effect of sand, high volume class C fly ash on thermal conductivity of the oven-dried pastes and mortars. Fly ash was used to replace cement at 50% and 70% for both pastes and mortars. He found that sand increased thermal conductivity of cement paste up to 83%. Thermal conductivity decreased with the increase of fly ash about 54% and 60% for mortar and paste.

Demirboğa (2003) investigated the effect of class C fly ash on mortar. Fly ash was used to replace cement in the ratios of 0.1, 0.2 and 0.3 by weight. The samples were tested in the oven-dried condition at 28 days of age. Thermal conductivity decreased with the increase of fly ash content.

Demirboğa (2007) studied the effect of fly ash on thermal conductivity of concrete. Fly ash was used to replace cement in the ratios of 0.15 and 0.30 by weight. The samples were tested in the oven-dried condition at 28 days of age. Thermal conductivity decreased with the increase of fly ash content. Thermal conductivity of concrete decreased 12 and 23% when the percentage of fly ash replacement were 15 and 30%, respectively, compared to the control specimens (100% Portland cement).

Demirboğa et al. (2007) reported the results of a study conducted to evaluate the influence of high volume class C fly ash on thermal conductivity of concrete. Thermal conductivity of concrete decreased 32, 33 and 39% for 50, 60 and 70% fly ash replacement of cement, respectively, compared to the control specimens (100% Portland cement).

Bentz (2007) conducted experiments to measure thermal conductivity of cement pastes since fresh state until 28 days at 20 ^{o}C. The transient plane source measurement technique, Hot Disk Thermal Constants Analyzer, was used in his study. Variables investigated included w/b and curing condition (sealed and saturated curing). The measured thermal conductivities of fresh pastes along with the known thermal conductivity of water are used to estimate thermal conductivity of the cement powder. He found that the hydration had only a minor influence on the measured thermal conductivity. The thermal conductivity of cement powder was found to be 1.55 W/ (m K).

2.1.3 Convection heat transfer coefficient at the surface of concrete

Convection is the mode of heat transfer associated with fluid or air motion. For mass concrete, the rate of heat flow from a horizontal surface is controlled by the magnitude of the temperature difference, the wind speed, and the surface texture of concrete. In case of heat transfer to the air by natural convection (wind speed equals to zero), the heat transferred by convection is found to be proportional to temperature difference. The expression for heat convection which is known as Newton's law of cooling, is shown in Eq. (2.4).

$$q_c = h_c (T - T_{sur}) \tag{2.4}$$

where q_c is the heat flow from the surface into the fluid or air (W/hr). ΔT is the temperature gradient between surface of concrete and enviroment (^{o}C). h_c is the average convection heat transfer coefficient (W/m^2 ^{o}C) .

The wind velocity influences the temperature gradient of concrete to air interface (solid to fluid interface), then the wind speed influences h_c. The greather wind speed the higher heat transfer from concrete to air. As heat is transferred from the warmer horizontal member to the adjacent air, the air is heated, its density decreases, and it tends to rise. As the heated air rises, it is replaced by cooler air that, in turn, is heated and rises. This is a continuous reoccurring

process, repeating itself until the heat balance is eliminated. This complex phenomenon has been thoroughly investigated by numerous researches in the heat transfer field.

William (1986) stated that the convection coefficient depended on the temperature gradient between the surface and the ambient air. The velocity of air influences the convection heat transfer coefficient. He proposed that the value of convection heat transfer coefficient for air in natural convection between 5 to 25 W/(m^2 K) be used as a guide to obtain an estimation.

U.S. Army Corps of Engineer (1997) proposed the surface heat transfer coefficient for the concrete surface with and without foam or insulation. For surface without insulation, the model was computed based on the wind speed. The wind velocity may be based on monthly average wind velocity at the project site. The proposed model is shown in Eq. (2.5) and (2.6).

$$h = aV^b \qquad \text{for } V > 17.5 \text{ km/h} \qquad (2.5)$$

$$h = c + dV \qquad \text{for } V < 17.5 \text{ km/h} \qquad (2.6)$$

where h is the surface heat transfer coefficient for surface without insulation (W/m^2 ^oC), a, b, c and d are the constants equal to 2.6362, 0.8, 5.622 and 1.086 respectively. V is the wind velocity (km/h)

For concrete surface with insulation, Eq. (2.7) was proposed. The value of h from the equation above was revised. The revised heat transfer coefficient was proposed based on the thermal conductivity of the insulation material.

$$h' = \frac{1}{\left(\frac{b}{k}\right)_{formwork} + \left(\frac{b}{k}\right)_{insulation} + \left(\frac{1}{h}\right)} \qquad (2.7)$$

where h' is the revised surface heat transfer coefficient (W/m^2K), b is the thickness of formwork or insulation (m) and k is the conductivity of formwork or insulation (W/mK).

Schlangen (2000) proposed the convection coefficient for concrete surface which was calculated based on the wind speed and the following equations were used in his calculation

$$h_c = 5.6 + 4.0V_{wind} \qquad \text{for } V_{wind} < 5 \text{ m/s} \qquad (2.8)$$

$$h_c = 7.2V_{wind}^{0.78} \qquad \text{for } V_{wind} > 5 \text{ m/s} \qquad (2.9)$$

where V_{wind} is the measured wind speed (m/s).

Ruiz et al. (2001) proposed a model for use on a horizontal surface that is valid for both forced and free convection. The expression is shown in Eq. (2.10). Thermal convection is the heat transferred from a surface to fluid or gas due to the temperature difference. Convection is, therefore, the mechanism of heat transfer between the concrete surface and the environment. For pavements, wind velocity across the concrete surface determines whether

convection is forced or free. They also proposed a computer model for predicting the core concrete temperature of pavement. The model consists of a transient two-dimensional finite-element model and it also includes the effects of thermal conduction, convection, solar radiation, irradiation, and the heat of hydration of the cementitious materials.

$$h_c = 3.727C\left(0.9\left(T_s + T_a\right) + 31\right)^{-0.181}\left(T_s - T_a\right)^{0.266}\sqrt{\left(1 + 2.857V_{wind}\right)} \quad (2.10)$$

where h_c is surface convection coefficient (W/m^2 °C), C is a constant depending on the shape and heat flow condition, C is equal to1.79 for horizontal plates warmer than air and 0.89 for horizontal plates cooler than air, respectively, T_s is the surface temperature (°C) and T_a is the air temperature (°C)

Priestley and Thurston (1979) suggested the equation for calculating the surface heat transfer coefficient as a function of average wind speed. The expression is shown in Eq. (2.11).

$$h_c = 13.5 + 3.88V \quad (2.11)$$

where, h_c is surface convection coefficient (W/m^2 °C) and V is the average wind speed (m/s)

2.1.4 Radiation and irradiation

Solar absorption is the flux absorbed by the concrete surface through exposure to the incoming sunrays. A simple equation for the incoming heat flow due to this source is shown in Eq. (2.11) (Ruiz et al. 2001).

$$q_s = \beta_e \; q_{solar} \quad (2.12)$$

where q_s is the solar absorption heat flux (W/m^2), β_e is the solar absorptivity and q_{solar} is the instantaneous solar radiation, (W/m^2) as defined in Table 2.1.

It is noted in Table 2.1 that the solar radiation is a function of the cloud cover, and even with an overcast sky some of the longer wavelengths can still penetrate the sky and be a source of heat. During nighttime, the solar radiation is negligible. The solar absorptivity, $\beta_{e,}$ of Portland cement concrete is a function of the surface color, with typical values ranging from 0.5 to 0.6. An ideal white-body would have a value of 0.0, and an ideal black-body would have a value of 1.0.

Table 2.1: Solar radiation values.

Sky Conditions	Solar Radiation, q_{solar}, (W/m^2)
Sunny	1,000
Partly Cloudy	700
Cloudy (Overcast)	300

Irradiation heat transfer is accomplished by electromagnetic waves between a surface and its surroundings. The Stefan-Boltzmann law is commonly used for this type of heat transfer, which is defined as follows Eq. (2.13):

$$q_r = \varepsilon \quad \rho\left(T_c^4 - T_{sur}^4\right) \tag{2.13}$$

where, q_r is the heat flux of heat emission from the surface (W/m^2), ρ is the Stefan-Boltzmann radiation constant ($5.67x10^{-8}$ $W/m^2/°C^4$), ε is the surface emissivity of concrete, T_c is the concrete surface temperature (°C), and T_{sur} is the surrounding air temperature, (°C).

The surface emissivity is a function of the concrete surface color. An "idealized" black surface would have a value of 1.0. In many study, a value of 0.88 was selected for concrete. However, note that in the above equation T_{sur} is the temperature of the surrounding environment, and this value cannot arbitrarily be assumed to be equal to the ambient temperature.

Fig 2.1 shows the behaviors of heat transfer of concrete. Inside concrete, heat transfer from core zone to the surface by heat conduction process. Heat transfer from concrete to surrounding by heat convection process. During day time, concrete absorb heat from sunray and this process is solar absorption. The irradiation is the emission of radiation from warm concrete to its surrounding.

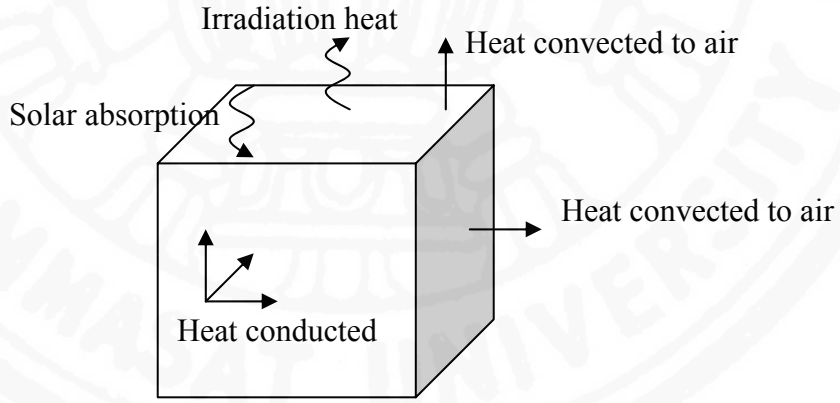

Fig 2.1 Behaviors of heat transfer of concrete

Burkan et al (2004) proposed the equation for calculating the total radiation absorbed by the concrete surface as shown in Eq. (2.14).

$$q_s = \alpha I_n \tag{2.14}$$

where, q_s is the total radiation absorbed, α is the absorbtivity of concrete, which varies between 0.5 and 1.0 depending on the color and the texture of the surface, and I_n is the direct solar radiation intensity which can be approximated by using Eq. (2.15)

$$I_n = C_N G_Z e^{(-\tau/\cos\beta)} \tag{2.15}$$

where, C_n is the clearness number, which depends on the location of the structure within the world, β is the solar zenith angle, G_Z and τ are given by the following trigonometric series.

$$\begin{aligned} G_z &= 1162.4 + 77.4\cos(C_T) - 3.6\cos(2C_T) - 3.4\cos(3C_T) \\ &+ 1.8\sin(C_T) - 0.6\sin(2C_T) + 0.9\sin(3C_T) \end{aligned} \tag{2.16}$$

$$\begin{aligned} \tau &= 0.1717 - 0.0344\cos(C_T) + 0.0032\cos(2C_T) + 0.0024\cos(3C_T) \\ &- 0.0043\sin(C_T) - 0.0008\sin(3C_T) \end{aligned} \tag{2.17}$$

where, $C_T=2\pi n_y/366$, n_y is the day of the year.

Burkan et al. (2004) also proposed the equation for calculating the irradiation from the concrete surface and can be obtained by using the Stefan-Boltzman law. The equation is the same as that proposed by Ruiz which is shown in Eq. (2.13) but the ratio of emission from gray surface is equal to 0.9.

2.1.5 Thermal expansion coefficient

Neville (1987) explains that concrete expands slightly as temperature rises and contracts as temperature falls, although it can expand slightly as free water in the concrete freezes. Temperature changes may be caused by environmental conditions or by cement hydration. The thermal coefficient of expansion (*CTE*) is a length change (expansion due to temperature increase and contraction due to a temperature decrease) in a unit length per a unit degree of temperature change. *CTE* is expressed in micron per degree Celsius. The expression of coefficient of thermal expansion is shown in Eq. (2.18).

$$CTE_c = (\Delta L/L_0) / \Delta T \tag{2.18}$$

where CTE_c is thermal expansion coefficient of concrete (micron/°C), ΔL is the length change of specimen due to temperature change (mm.), L_0 is the initial measured length of specimen (mm.), and ΔT is the temperature change (°C).

The thermal coefficient of expansion of concrete depends both on the composition of the mix and on its hygral state at the time of the temperature change. The coefficient of thermal expansion of concrete is a resultant of the coefficients of cement paste and aggregate since they are the main constituents of the concrete. The coefficient for concrete is affected by these two values and also by the volumetric proportions and elastic properties of the two constituents. The CTE_c is related to the thermal coefficient of aggregate, CTE_a, and of cement paste, CTE_p, as shown in Eq. (2.19).

$$CTE_c = CTE_p - \frac{2n\left(CTE_p - CTE_a\right)}{1 + \frac{k_p}{k_a} + n\left[1 - \frac{k_p}{k_a}\right]} \tag{2.19}$$

where CTE_c, CTE_a and CTE_p are thermal coefficients of concrete, aggregate and cement paste, respectively (micron/°C). n is volumetric content of aggregate and k_p/k_a is the stiffness ratio of cement paste to aggregate (MPa).

The coefficient of thermal expansion of cement paste varies between about 11 and 20 micron/°C. The thermal coefficient of expansion of concrete varies mainly with the character and amount of the coarse aggregate. Quartz has a coefficient about 12.6 micron/°C while some limestone have a value as low as 5.4 micron/°C. Moisture conditions and the relative humidity of ambient air also have an influence on the thermal expansion coefficient of concrete. It appears that the coefficients of thermal expansion of oven-dried and water-saturated concretes are approximately equal but that partly dried concrete has a higher coefficient.

Berwanger and Sarkar (1976) determined the thermal coefficient of expansion of concrete and reinforced concrete under short-term steady state temperature; -73 to 66 °C. Specimens were cured both saturated and air-dried in the laboratory and tested at 7, 28 and 84 days as well as at 1 year. They found that the coefficient decreased with increase in the w/b and increased with age.

ACI committee 517 (1988) stated that the coefficient of thermal expansion of fresh concrete is several times higher than that of the hardened concrete. It decreases sharply during the first ten hours of hydration and then remains constant

Kada et al. (2002) proposed a simple method to determine the coefficient of thermal expansion at early ages by applying temperature shock with the tested temperature range of 10 ^{o}C to 50 ^{o}C and the test duration of less than one hour. The effect of autogeneous shrinkage was neglected in his study because the test duration was short. They reported that the coefficient of thermal expansion of the concrete having a w/b of 0.45 decreased sharply from 32 to 6.5 micron/°C in a few hours and than remain almost constant at 6.5 micron/°C. A similar behavior was observed for the concrete with w/b of 0.35, whereas for the concrete having a w/b of 0.3 the coefficient of thermal expansion decreased from 13 to 7.6 micron/°C in six hours, to then remain constant at 7.6 micron/°C.

Yang and Sato (2002) proposed a method for measuring *CTE* of high strength concrete. They avoided autogeneous shrinkage strain during the measurement of thermal strain by reducing the hydration that occurred during the test period. The rate of hydration reaction was reduced by the decrease of concrete temperature to a very low level. The *CTE* excluding autogeneous shrinkage could be obtained by the use of temperature change in the very low temperature region and the range of temperature changes used in their study were between -1 ^{o}C to 5 ^{o}C. However, the method requires sophisticated equipment. *CTE* of high strength concrete decreased rapidly after setting and reached a minimum value at about 1 day. Thereafter, *CTE* increased with time up to the age of 7 days depending on the development of self-desiccation.

Gambhir (2004) states that the coefficient of thermal expansion of the concrete increases with the coefficient of thermal expansion of aggregate. If the coefficient of expansion of coarse aggregate and cement paste differs too much, a large change in temperature may introduce differential movement which may break the bond between the aggregate and the paste. The linear thermal coefficient of expansion of concrete lies in the range of 5.8 to 14 micron/°C depending upon the type of aggregate, mix proportions and degree of saturation.

Bjontegaard and Sellevold (2001) proposed another method to measure *CTE* of high performance concrete. The *CTE* was measured by using various temperature histories. The specimens were heated up by 7 ^{o}C to 10 ^{o}C per step until reaching the required temperature history. Thermal deformation was measured in each temperature step and autogeneous deformation was measured directly between each temperature step. The method is reasonable for measurement of the *CTE* by automatically deleting the effect of autogeneous shrinkage, but it requires relatively complicated facilities.

Neekhra (2004) introduced a new mineralogical approach model for predicting aggregate and concrete thermal expansion coefficient. The *CTE* of aggregate was calculated based on the determined *CTE* of pure minerals and their respective calculated volume percentages as shown in Eq.(2.20).

$$CTE_g = x\sum\left(CTE_i V_i\right) + \left(1-x\right)\left\{\frac{\sum\left(CTE_i V_i E_i\right)}{\sum\left(V_i E_i\right)}\right\} \tag{2.20}$$

where CTE_g and CTE_i are the CTE of coarse aggregate and individual mineral in aggregate (micron/°C). V_i is the volume fraction of each mineral in aggregate. E_i is the modulus of elasticity of each mineral phase (MPa). x is the relative portions of mineral conforming with the upper and lower bound solution (in his study a value of 0.5 is used).

CTE of concrete is determined based on the *CTE* of mortar and coarse aggregate as shown in Eq. (2.21)

$$CTE_c = x\left(CTE_m V_m + CTE_g V_g\right) + \left(1-x\right)\frac{CTE_m V_m E_m + CTE_g V_g E_g}{V_m E_m + V_g E_g} \tag{2.21}$$

where CTE_c, CTE_m and CTE_g are the *CTE* of concrete, mortar and coarse aggregate, respectively (micron/°C). V_m and V_g are the volume fraction of mortar and coarse aggregate. E_m and E_g are the modulus of elasticity of mortar and coarse aggregate, respectively (MPa).

Concretes prepared with many types of aggregate, such as limestone (LST1, 6 and 9), sandstone (SST-12), siliceous gravel (SRG -1, 2 and 3) and calcareous gravel (CRG-3). The testes were conducted at the age of 28 days. The predicted *CTE* of concrete and the measured *CTE* of concrete show good correlation.

ACI committee 209 (1992) proposed an equation for predicting *CTE* based on the degree of saturation and *CTE* of aggregate as shown in Eq. (2.22). However, for ordinary thermal stress calculation, when the type of aggregate and concrete degree of saturation are unknown the value of 10 micron/°C may be sufficient.

$$CTE_c = CTE_{mc} + 3.1 + 0.72\ CTE_g \tag{2.22}$$

where CTE_{mc} is the corrected *CTE* based on the degree of saturation of concrete member (micron/°C). CTE_g is the *CTE* of coarse aggregate

2.1.6 Thermal stress and tensile strain capacity of concrete

Ivan E. Houk, Jr., Jame A. Paxton, and Donald L. Houghton (1970) investigated tensile and compressive strain of plain concrete beam. The flexural strength of plain concrete beams ranged from 13 to 28 percent of the compressive strength of 15×30 cm. cylinders. Unit strain sustained by concrete near failure loading increased with age and strength of concrete.

Houghton (1976) proposed a rapid test method for estimating tensile strain capacity of mass concrete. Tensile strain capacity was measured by flexural test on plain beams simply supported and loaded at the third points. Tensile strain capacity under rapid loading is estimated using the modulus of elasticity and rupture of concrete but the creep properties are needed in the estimation of strain capacity under slow loading. He found that tensile strain capacity of concrete was increased significantly by using crushed aggregate and milled sand and by increasing cement content. Utilization of crushed and milled aggregate increased the strain capacity 50 % under rapid loading test and from 40% to 85 % under slow loading test.

Troxell, Davis and Kelly (1968) described the relationship between compressive and direct tensile strength of concrete. The tensile strength ranges from 7 to 11 % of the compressive strength and the modulus of rupture ranges from 11 to 23 % of the compressive strength. The modulus of rupture ranges from 60 to 100 % higher than the direct tensile strength.

Bach (1986) reported the relationship between flexural and tensile strength. When using fly ash as a partial or complete substitution for Portland cement. Data obtained from both laboratory experiments and field experiments generally indicate that flexural strength and splitting tensile strength can be predicted from compressive strength results. The ratio of

flexural to compressive strength is generally found to be slightly higher than the ratio of indirect tensile to compressive strength.

Schubert (1986) reported the effect of fly ash on deformation behavior in tension. Ultimate tensile strain at early ages is less for fly ash than for non-fly-ash concretes, but the difference decreases with time. Eventually, the ultimate strain of concretes containing fly ash is greater than that of concretes without fly ash. The ultimate tensile strain increases with higher cement and fly ash contents, but reduces due to using excessive amounts of fly ash.

Jitvutikrai (2000) conducted the experiments on splitting tensile strength under different curing temperature. The experiments were conducted by varying fly ash replacement ratios (r) at 0, 0.2, 0.4 and 0.6, water to binder ratios (w/b) at 0.4 and 0.6 and curing temperature at 30 °C, 50 °C and 65 °C. He found that fly ash content has no clear tendency to affect the splitting tensile strength of the tested concrete under the tested curing temperature. For the effect of curing temperature, it seems to have a tendency that concrete subjected to 65 °C curing temperature has higher splitting tensile strength than those cured at 30 °C and 50 °C. But curing temperature at 50 °C does not result in much difference when compared to the curing condition at 30 °C.

Wee et al. (2000) conducted testes on direct tension, compression, modulus of elasticity and flexural strength of concrete. Tensile strain capacity of concrete was investigated by using flexural test and direct tension test. It was found that tensile strain capacity of concrete is between 150 με and 210 με in the flexural-strength test and between 100 με and 140 με in the direct tension test. Tensile strength obtained from the direct tension test is about two-thirds of the flexural strength of concrete. Flexural strength is about 8 to 11.5 % of the cylinder compressive strength or 6.5 to 9.5 % of the cube strength. Tensile strength is 5.5 to 8.5% of the cylinder compressive strength or 4.5 to 7% of the cube strength. The modulus of elasticity obtained from the tension test is similar to that obtained from compressive test for low-grade concrete but the values of tension test are lower than those of compressive test for concrete of high grade.

Lu et al. (2001) evaluated thermal crack by a probabilistic model using the tensile strain capacity. The model was formulated from the results of 215 tensile specimens of concrete. Direct tension test was used in their study. Tensile strain capacity is estimated from the tensile strain at failure. The mean and the standard deviation of the test results are 111 με and 17 με, respectively. In other word, when the restrained strain reaches 111 με, the probability of occurrence of a crack is 50%. The model was verified with the experiments. Eight cylinders with different mixes of concrete were cast and the testes were done at various ages. An aluminum heater was embedded into the center of each specimens and temperature distribution was measured along the radius by using thermocouples. Tensile strain on the surface induced by restraint is calculated from temperature distribution at cracking. Since the test period is short (about 10 min) then the effect of shrinkage and creep are neglected. The probability of the occurrences of a crack is evaluated by the probabilistic model. It was found that when the probability is over 50% or the tensile strain on surface is more than 111 με, concrete tends to crack.

Kim et al. (2002) conducted experiments on strength and modulus of elasticity of concrete with different curing temperature and age. Tests of 480 cylinders made of types I, V, and type V cement - fly ash concretes, cured in isothermal conditions of 10, 23, 35, and 50 ^{o}C and tested at the ages of 1, 3, 7, and 28 days. They found that concretes subjected to high temperatures at early ages attain higher early age compressive and splitting tensile strengths but lower later age compressive and splitting tensile strengths than concretes subjected to normal temperature. Cement type (Types I and V cement), curing temperature (from 10 to 50 ^{o}C), and age (less than 28 days) have no large effects on the relationship between elastic modulus and compressive strength and the relationship between splitting tensile strength and compressive strength.

Swaddiwudhipong et al. (2003) conducted the experiments on tensile strain capacity of concrete under uniaxial tension. The direct tension test method was used in their study. Seven mixes of concrete were designed to study the effect of age, compressive strength and mineral admixture. They found that tensile strain capacity of concrete was a relatively independent parameter. The mix proportion, curing age and concrete compressive strength did not seem to affect significantly the tensile strain at failure and at 90% failure load. The average tensile strains at failure and 90% failure load were 120 and 100 με, respectively.

Tongaroonsri and Tangtermsirikul (2008) conducted experiments to investigate the tensile strain capacity of concrete. The effect of water to binder ratio, paste content, type of cement, content of mineral admixtures, aggregate maximum size, sand content and presence of moisture on tensile strain capacity of concrete were investigated using flexural test method. The mineral admixtures used in their study were fly ash, ground granulated blast-furnace slag and two types of limestone powder having different fineness (fine grain and coarse grain) with the average particle size of 2 and 13 micron, respectively. It was found that tensile strain capacity of concrete increased with age due to increase of strength. The effect of cement type, paste content and s/a in their tested range was not significant. Cracking strain decreased with the increase of w/b, replacement ratio of fly ash and limestone powder. For ground granulated blast-furnace slag (GGBS), specimens containing 30% and 50% GGBS showed higher cracking strain than that without GGBS but at 70% GGBS, cracking strain decreased. Cracking strain of high w/b concrete (w/b=0.55) was the highest when G_{max} was 19 mm. However, when w/b was 0.30, there was a tendency that cracking strain was the highest when G_{max} was 10 mm. Cracking strain increased whereas flexural strength and splitting tensile strength reduced when concrete was oven-dried.

2.2 Effect of Fly Ash on Heat Evolution of Concrete

Kokubu (1969) found that the initial rate of heat evolution of the mixture of cement-fly ash paste increased progressively with increasing fly ash content in spite of the decreased cement contents. This was attributed not to reaction of the fly ash but to acceleration of cement hydration. If the pozzolan is highly active then the heat of reaction of the pozzolan is also contribute to the heat evolution in the early stages of reaction, compensating for the reduction in the cement content. Thus the combination of acceleration in cement hydration and the pozzolanic reaction can lead to enhanced rates of early heat evolution and a subsequent temperature rise in excess of that for Portland cement alone.

Tokyay (1988) investigated the effects of the type and amount of fly ash substitution on the heat of hydration of Portland cement-fly ash pastes. The results revealed that the high-calcium fly ash was not as effective as the low-calcium ones in reducing the early heat of hydration of the Portland cement-fly ash systems. He also reported that high levels of fly ash substitutions significantly reduced the early age heat evolution.

Atis (2002) studied heat evolution of high-volume fly ash (HVFA) concrete by measuring the temperature increase in concrete under adiabatic curing condition. He found that using fly ash as cement replacement resulted in a reduction on the maximum temperature rise. Increasing the replacement level of fly ash caused lower temperature rise of concrete.

Bai and Wild (2002) investigated the temperature change and heat evolution of mortar incorporating fly ash. Temperature-time profiles of mortar cubes have been determined using a semi adiabatic curing method for curing times of 160 h. Each mortar mix was placed in a 150 mm plywood cube mould that was fully encased in 100 mm thick expanded polystyrene within an outer 400 mm plywood cube. They found that the temperature rise in cement-fly ash mortars is less than that in an equivalent cement mortar. This is attributed to the dilution of the cement by fly ash coupled with the latter's negligible pozzolanic activity during the early stages of hydration, thus reducing both the rate of heat evolution and the total heat evolved.

Langan et al. (2002) conducted the calorimeter tests on Portland cement-silica fume-fly ash mixtures. They reported that fly ash increased the initial hydration of cement due to more water is available for the initial hydrolysis. However, it retarded hydration in the dormant and acceleration periods. Fly ash retarded cement hydration more significantly at high water to cementitious ratios. When silica fume and fly ash are incorporated together in cement, the hydration of the cement is significantly retarded. The heat of hydration is decreased and the early reactivity of the silica fume is hampered. The accelerating effect of the silica fume is delayed.

2.3 Model for Predicting Temperature Rise and Thermal Cracking due to Heat of Hydration.

Koenders and Breugel (1994) determined the adiabatic hydration curves by assuming a linear relationship between the degree of hydration and the liberated heat of hydration and that all the liberated heat was used for heating up of the hydrating sample. The hydration curves can be calculated as a function of the clinker composition of the cement and the mix composition of the concrete. The adiabatic hydration curves of concrete mixes were used as input for computer programs utilized for the calculation of the temperature distribution in hardening concrete. In their calculations the specific heat of the concrete was considered to be a function of the degree of hydration.

Wang and Dilger (1994) developed a computer model for predicting temperature distribution in hardening concrete. A two-dimensional finite element thermal analysis was employed to model the transient heat transfer between the concrete and the surroundings as affected by the concrete mix, thermal boundary and environmental conditions. They stated that the cement hydration heat rate at standard temperature (20°C) and other temperature could be derived by the test results on adiabatic temperature rise with time for the concrete mix.

Kishi and Maekawa (1996) proposed the multi-component model for hydration heat of blended cement. Four clinker minerals of Portland cement, blast furnace slag, and fly ash were taken up as the reactive components. In their model, the referential heat rate and the thermal activity of each mineral constituent were identified as the material functions. The hydration degree of each mineral compound of Portland cement as well as the pozzolans was computed step by step with modified Arrhenius's law of chemical reaction. The conversion of ettringite to monosulphate was also combined in the model. Their model was verified through the analysis of the adiabatic and semi-adiabatic temperature rises.

Bentz et al. (1998) prepared a series of conventional and high-performance concretes, with and without silica fume additions and characterized with respect to their adiabatic heat signature. The NIST 3-D microstructure model was used to compare with the measured responses. Their model incorporated the pozzolanic reaction of silica fume and was used to simulate hydration under adiabatic conditions. The model was based on the activation energies and heat of reaction for the hydration and pozzolanic reactions and the heat capacity of the hydrating concrete mixture.

Sarker et al. (1999) applied a model for predicting temperature rise in concrete using fly ash. The computerized program proposed by Kishi and Maekawa (1996) was modified to be used for various types of fly ashes. In the fly ash model, the reference heat rate and thermal activity of different types of fly ashes were expressed as functions of their CaO content. Temperature rise values in concrete specimens and a mat footing were compared using the proposed models with the measured results. Good correlation among the analytical and test results was obtained.

Saengsoy and Tangtermsirikul. (2003) proposed a computerized program for predicting temperature of mass concrete in the adiabatic condition. The cumulative heat was computed based on the summation of the heat liberated from the reaction of each cement compound including the formation of ettringite and monosulphate, and the reaction of fly ash. The specific heat model considering time dependent properties was adopted for relating the heat generated in the concrete and its temperature rise to achieve more realistic temperature simulation especially during early age of mass concrete. The accuracy of the model was evaluated by comparing the computed temperature by the proposed model with the test results of adiabatic temperature of cement only and fly ash concrete. It was found that the formulated model could accurately predict the test results.

Ballim (2004) developed a finite difference heat model for predicting the temperature in mass concrete elements. The model represents a two-dimensional solution to the Fourier heat flow equation and runs on a commercially available spreadsheet package. An adiabatic calorimeter was developed and built to measure the rate of heat evolution of concrete mixture to be used in concrete element. The maturity based heat rate curve was used as input into the numerical model. The model was verified with a concrete block cast in the laboratory. The results show that the model is able to predict the temperature at any point in concrete block to within 2 ^{o}C of the measured values.

Buffo-Lacarrier et al. (2007) proposed a model for predicting the development of hydration and its consequences on temperature and water content. The hydration model was applicable for cement and other mineral additions (fly ash and silica fume). The hydration degree of each anhydrous phase was modeled as a function of thermal activation, chemical activation and water accessibility to anhydrous phase. The constant thermal properties of concrete were used in their study. The model was tested on a 27 m^3 concrete block in situ equipped with temperature sensors situated in the core and close to the face exposed to solar radiation. The analytical results showed good agreement with experimental results.

Park et al. (2008) developed of a computational program to predict the temperature history in high-strength concrete members. The numerical simulation procedure was started with a hydration model that describes the evolution of cement paste microstructure as a function of the changing composition of the hydration products. The cement paste was modeled as a unit cell that consists of three portions: the unhydrated cement grain, gel, and capillary pores. The coefficients for the hydration model were determined with an artificial neural network technique. Temperature distribution and history in concrete members considering thermal conductivity and radiant heat were calculated based on a three-dimensional mesh. Predicted temperature history curves were compared with experimental data and a good correlation was found. However, the proposed model cannot predict the temperature history of concrete, which includes mineral admixtures such as fly ash, slag, and silica fume, because a mathematical model does not solve the hydration and microstructure development of their effects.

Schutter (2002) proposed a model to simulate early age thermal cracking due to the heat of hydration. The proposed model based on the degree of hydration reaction. The developed hydration model was for Portland cement and blended cement like blast furnace slag cement. The cracking behavior was implemented using a smeared cracking approach with non-linear softening behavior. The time dependent material behavior is implemented in the model. In the analysis, specific heat and thermal diffusivity of hardening concrete decreases linearly with the increasing of degree of hydration. Mechanical behavior of harden concrete such as compressive strength, tensile strength, modulus of elasticity, poisson's ratio, fracture energy and creep is intensively related with the degree of hydration. It was mentioned in his study that coefficient of thermal expansion was also evolving during the hydration of concrete but by lack of experimental results, a constant value was used in his study. The analytical results were verified with the experimental results of a concrete prism with section 150 mm. x 150 mm. The proposed model was also verified with a cracked concrete armour unit. The simulation results show good agreement with experimental results.

Faria et al. (2006) presented a thermo-mechanical model based on the framework of finite element techniques with the consideration of phenomena such as the heat production induced by the cement hydration, the evolving properties of concrete during hydration and early-age creep. A numerical application was presented, focused on the thermo-mechanical behaviour of a slab strongly restrained by the supporting piles, which had been monitored during the construction phase. The thermal problem arising from the cement hydration reaction included an Arrhenius law for the internal heat source, and it was solved by adopting a finite element spatial discretization and a backward-Euler time integration scheme. The mechanical problem that was arisen from the non-uniform thermal field was solved by the

finite element method, taking into consideration the changes in the mechanical properties of concrete due to ageing, creep and shrinkage phenomena. Thermo-mechanical model provided results that were well correlated with the observed in situ measurements of temperatures and strains.

Kwak et al. (2006) introduced a three-dimensional finite element model for the analysis of non-structural cracks occurring in reinforced concrete (RC) walls. The numerical model could take into account time-dependent temperature variations due to hydration heat and non-uniform moisture distribution during drying. The coupling effect between the heat transfer and the moisture diffusion were also considered in the model. Calculation of the temperature and internal relative humidity variations of RC walls was followed by determination of stresses due to thermal gradients, differential drying shrinkage, and average drying shrinkage. The mechanical properties of early age concrete were determined from numerous experimental studies. The proposed model could effectively be used to quantitatively estimate the occurrence of non-structural cracking in RC walls.

Kwak and Ha (2006) proposed an improved analytical mode for a quantitative assessment of non-structural cracking in reinforced concrete (RC) wall. By using the proposed model, the influence of changes in the material properties and construction conditions such as the effect of casting temperature, effect of casting length and effect of temperature steel on the cracking in RC walls were investigated. In the calculation of temperature steel, they suggested that the ACI 207 provides a reasonable guide to control cracking in RC walls. The properly placed with adequate amounts of reinforcement could prevent unsightly cracking. The cracks were distributed in such a way that a larger number of very fine cracks occurred instead of a few wide cracks.